

# Dark photon dark matter in quantum electromagnetodynamics and detection at haloscope experiments\*

Chang-Jie Dai (代昌杰)<sup>†</sup> Tong Li (李佟)<sup>\*\*</sup> Rui-Jia Zhang (张瑞珈)<sup>§</sup>

School of Physics, Nankai University, Tianjin 300071, China

**Abstract:** The ultralight dark photon is an intriguing dark matter candidate. The interaction between visible and dark photons is introduced by the gauge kinetic mixing between the field strength tensors of the Abelian gauge groups in the Standard Model and dark sector. Relativistic electrodynamics was generalized to quantum electromagnetodynamics (QEMD) in the presence of both electric and magnetic charges. The photon is described by two four-potentials corresponding to two  $U(1)$  gauge groups and satisfying non-trivial commutation relations. In this work, we construct low-energy dark photon-photon interactions in the QEMD framework and obtain new dark photon-photon kinetic mixings. Then, we derive the consequent field and Maxwell's equations. We also investigate the detection strategies of dark photons as light dark matter and generic kinetic mixings at haloscope experiments.

**Keywords:** dark photon, quantum electromagnetodynamics, haloscope detection

**DOI:** 10.1088/1674-1137/adbd19 **CSTR:** 32044.14.ChinesePhysicsC.49053105

## I. INTRODUCTION

The numerous candidates of dark matter (DM) have motivated the search for potential hidden particles in a wide range of mass scales. The dark photon (DP), also called the hidden photon, [1, 2] is an appealing candidate of ultralight bosonic DM [3–5] (see a recent review Ref. [6] and references therein). It is a spin-one field particle gauged by an Abelian group in the dark sector. The visible and dark photons interact through the gauge kinetic mixing between the field strength tensors of Standard Model (SM) electromagnetic gauge group  $U(1)_{\text{EM}}$  and dark Abelian gauge group  $U(1)_D$  below the electroweak scale

$$\mathcal{L} \supset -\frac{1}{4}F^{\mu\nu}F_{\mu\nu} - \frac{1}{4}F_D^{\mu\nu}F_{D\mu\nu} - \frac{\epsilon}{2}F^{\mu\nu}F_{D\mu\nu} + \frac{1}{2}m_D^2 A_D^\mu A_{D\mu}, \quad (1)$$

where  $F^{\mu\nu}$  ( $F_D^{\mu\nu}$ ) is the SM (dark) field strength and  $A_D$  is the dark gauge boson with mass  $m_D$ . If the SM particles are uncharged under the dark gauge group, kinetic mixing  $\epsilon \ll 1$  is generated by integrating new heavy particles charged under both gauge groups at loop level. The two

gauge fields can be rotated to get rid of the mixing. Consequently, the SM matter current shifts by  $A_\mu \rightarrow A_\mu - \epsilon A_{D\mu}$ . Based on quantum electrodynamics (QED), the electromagnetic signals from the source of dark photon DM can be searched for in terrestrial experiments [4, 7–17].

The description of relativistic electrodynamics may not be as simple as the QED theory. The magnetic monopole is one of the most longstanding and mysterious topics in history [18–26]. In the 1960s, J. S. Schwinger and D. Zwanziger developed generalized electrodynamics with monopoles in the presence of both electric and magnetic charges, called quantum electromagnetodynamics (QEMD) [27–29]. The characteristic feature of QEMD is the substitution of the  $U(1)_{\text{EM}}$  gauge group by two  $U(1)$  gauge groups to introduce both electric and magnetic charges. Two four-potentials  $A_\mu$  and  $B_\mu$  (instead of only one  $A_\mu$  in QED) are introduced corresponding to the two  $U(1)$  gauge groups  $U(1)_A$  and  $U(1)_B$ . They formally built a local Lagrangian density, a non-trivial form of equal-time canonical commutation relations that results in Lagrangian field equations in a local quantum field theory. Zwanziger *et al.* also proved that this theory preserves the

Received 4 November 2024; Accepted 6 March 2025; Published online 7 March 2025

\* Li Tong is supported by the National Natural Science Foundation of China (12375096, 12035008, 11975129)

<sup>†</sup> E-mail: daichangjie@mail.nankai.edu.cn

<sup>‡</sup> E-mail: litong@nankai.edu.cn (Corresponding author)

<sup>§</sup> E-mail: zhangruijia@mail.nankai.edu.cn

<sup>#</sup> These authors contributed equally as the first authors



Content from this work may be used under the terms of the Creative Commons Attribution 3.0 licence. Any further distribution of this work must maintain attribution to the author(s) and the title of the work, journal citation and DOI. Article funded by SCOAP<sup>3</sup> and published under licence by Chinese Physical Society and the Institute of High Energy Physics of the Chinese Academy of Sciences and the Institute of Modern Physics of the Chinese Academy of Sciences and IOP Publishing Ltd

right degrees of freedom for a physical photon and does not violate Lorentz invariance [30–32]. Recently, QEMD was used to point out that more generic axion-photon interactions may arise, and a few studies investigating their theory [32–35] and phenomenology [12, 36–42] have been published. As a result of axion-monopole dynamics, more anomalous axion-photon interactions and couplings arise in contrary to the ordinary axion-photon coupling. Our previous work investigated the new axion-modified Maxwell equations and analytically obtained the axion-induced electromagnetic fields [36]. Based on the solutions we obtained, we proposed new strategies to probe the new couplings of axion in LC circuit experiments [36], cavity experiments [39], interface haloscope experiments [38], and superconducting radio frequency cavity experiments [42]. This article aims to extend the closely related study to the field of DP in QEMD.

In this work, we construct the dark photon-photon interactions in the framework of QEMD and investigate the relevant detection strategies of light dark photon DM. We introduce new heavy fermions  $\psi$  charged under the four electromagnetic  $U(1)$  groups, that is,  $U(1)_A \times U(1)_B$  in the visible sector and  $U(1)_{A_D} \times U(1)_{B_D}$  in the dark sector. The covariant derivative of the  $\psi$  fermion in the kinetic term is then given by

$$i\bar{\psi}\gamma^\mu D_\mu\psi = i\bar{\psi}\gamma^\mu(\partial_\mu - eq_\psi A_\mu - gg_\psi B_\mu - eq_{D\psi} A_{D\mu} - gg_{D\psi} B_{D\mu})\psi, \quad (2)$$

where  $A_\mu, B_\mu$  ( $A_{D\mu}, B_{D\mu}$ ) are the potentials in the visible (dark) sector multiplied by the corresponding electric and magnetic charges. The visible photon is described by the two four-potentials  $A_\mu, B_\mu$  in the visible sector, and the dark photon is gauged under either QED (with only  $A_{D\mu}$ ) or QEMD (with both  $A_{D\mu}$  and  $B_{D\mu}$ ) in the dark sector. After integrating out the new fermions  $\psi$  in vacuum polarization diagrams of the four potentials, one can obtain the new kinetic mixings between dark and visible photons. We show their low-energy Lagrangian and the consequent field equations that are equivalent to new Maxwell's equations of dark photons. Based on the new Maxwell's equations, we also study the detection strategies through haloscope experiments to search for the light dark photon DM in this framework as well as the new kinetic mixings.

Some literature has also reported the kinetic mixing between two Abelian gauge theories that have both electric and magnetic charges [43–46]. However, in contrast to the ordinary kinetic mixing of the visible photon to the dark photon  $F_{\mu\nu}F_D^{\mu\nu}$  that they focused on, in this work, we build a complete low-energy Lagrangian of two Abelian gauge fields in both the visible and dark sectors and introduce an additional kinetic mixing between dark and visible photons. The complete low-energy Lagrangian with

this new kinetic mixing and a two-component DP DM scenario induce intriguing phenomenologies as we will discuss below.

This paper is organized as follows. In Sec. II, we introduce the QEMD theory and the effective Lagrangian of dark and visible photons in the QEMD framework. In Sec. III, we show the generic kinetic mixing terms in the Lagrangian. The consequent field equations and the new Maxwell's equations are then derived in the QEMD framework. We discuss the setup and signal power of haloscope experiments for the generic kinetic mixings and dark photon DM in Sec. IV. We also show the sensitivity of haloscope experiments to each kinetic mixing or dark photon DM component. Our conclusions are drawn in Sec. V.

## II. FORMALISM OF PHOTON AND DARK PHOTON IN QEMD FRAMEWORK

In this section, we first describe the QEMD theory and then introduce the necessary ingredients for constructing the extended dark photon-photon interactions based on QEMD.

To properly develop relativistic electrodynamics in the presence of magnetic monopole, introducing two four-potentials  $A_\mu$  and  $B_\mu$  corresponding to two  $U(1)$  gauge groups  $U(1)_A$  and  $U(1)_B$ , respectively [27–29], is the most reliable approach. Both the electric and magnetic charges are inherently brought into the same theoretical framework. The general Maxwell's equations in the presence of electric and magnetic currents are

$$\partial_\mu F^{\mu\nu} = j_e^\nu, \quad \partial_\mu F^{d\mu\nu} = j_m^\nu, \quad (3)$$

where the Hodge dual of field strength  $F^{\mu\nu}$  is  $F^{d\mu\nu} = 1/2\epsilon^{\mu\nu\rho\sigma}F_{\rho\sigma}$  with  $\epsilon_{0123} = +1$ , and the currents are conserved, with  $\partial_\mu j_e^\mu = \partial_\mu j_m^\mu = 0$ . The general solutions to the above equations are

$$F = \partial \wedge A - (n \cdot \partial)^{-1} (n \wedge j_m)^d, \quad (4)$$

$$F^d = \partial \wedge B + (n \cdot \partial)^{-1} (n \wedge j_e)^d, \quad (5)$$

where  $n^\mu = (0, \vec{n})$  is an arbitrary space-like vector, the integral operator  $(n \cdot \partial)^{-1}$  satisfies  $n \cdot \partial (n \cdot \partial)^{-1} (x) = \delta^4(x)$ , and  $(X \wedge Y)^{\mu\nu} \equiv X^\mu Y^\nu - X^\nu Y^\mu$  is defined for any four-vectors  $X$  and  $Y$ . The above field strength tensors satisfy

$$n \cdot F = n \cdot (\partial \wedge A), \quad n \cdot F^d = n \cdot (\partial \wedge B). \quad (6)$$

Using the identity  $G = (1/n^2)[(n \wedge (n \cdot G)) - (n \wedge (n \cdot G^d))^d]$  for any antisymmetric tensor  $G$ , one can rewrite  $F$  and  $F^d$

only in terms of potentials

$$F = \frac{1}{n^2}(n \wedge [n \cdot (\partial \wedge A)] - n \wedge [n \cdot (\partial \wedge B)]^d), \quad (7)$$

$$F^d = \frac{1}{n^2}(n \wedge [n \cdot (\partial \wedge A)]^d + n \wedge [n \cdot (\partial \wedge B)]). \quad (8)$$

After substituting them into Eq. (3), we obtain the Maxwell's equations

$$\frac{n \cdot \partial}{n^2}(n \cdot \partial A^\mu - \partial^\mu n \cdot A - n^\mu \partial \cdot A - \epsilon_{\nu\rho\sigma}^\mu n^\nu \partial^\rho B^\sigma) = j_e^\mu, \quad (9)$$

$$\frac{n \cdot \partial}{n^2}(n \cdot \partial B^\mu - \partial^\mu n \cdot B - n^\mu \partial \cdot B + \epsilon_{\nu\rho\sigma}^\mu n^\nu \partial^\rho A^\sigma) = j_m^\mu. \quad (10)$$

These Maxwell's equations can be realized by the local Lagrangian of a photon [29]:

$$\begin{aligned} \mathcal{L}_P = & -\frac{1}{2n^2}[n \cdot (\partial \wedge A)] \cdot [n \cdot (\partial \wedge B)]^d \\ & + \frac{1}{2n^2}[n \cdot (\partial \wedge B)] \cdot [n \cdot (\partial \wedge A)]^d \\ & - \frac{1}{2n^2}[n \cdot (\partial \wedge A)]^2 - \frac{1}{2n^2}[n \cdot (\partial \wedge B)]^2 \\ & - j_e \cdot A - j_m \cdot B + \mathcal{L}_G, \end{aligned} \quad (11)$$

where  $\mathcal{L}_G = (1/2n^2)\{[\partial(n \cdot A)]^2 + [\partial(n \cdot B)]^2\}$  is a gauge fixing term. One can rewrite it in terms of canonical variables and obtain the non-trivial commutation relations between the two four-potentials [29]:

$$[A^\mu(t, \vec{x}), B^\nu(t, \vec{y})] = i\epsilon_{\alpha 0}^{\mu\nu} n^\alpha (n \cdot \partial)^{-1}(\vec{x} - \vec{y}), \quad (12)$$

$$\begin{aligned} [A^\mu(t, \vec{x}), A^\nu(t, \vec{y})] &= [B^\mu(t, \vec{x}), B^\nu(t, \vec{y})] \\ &= -i(g_0^\mu n^\nu + g_0^\nu n^\mu)(n \cdot \partial)^{-1}(\vec{x} - \vec{y}). \end{aligned} \quad (13)$$

The right number of photon degrees of freedom is preserved due to the constraints from the above equations of motion, gauge condition, and equal-time commutation relations. We notice the other important identity between two antisymmetric tensors  $G$  and  $H$

$$\text{tr}(G \cdot H) = G^{\mu\nu} H_{\nu\mu} = \frac{2}{n^2}[-(n \cdot G)(n \cdot H) + (n \cdot G^d)(n \cdot H^d)]. \quad (14)$$

The QEMD Lagrangian of the visible photon is then rewritten as

$$\mathcal{L}_P = \frac{1}{4}\text{tr}(F \cdot (\partial \wedge A)) + \frac{1}{4}\text{tr}(F^d \cdot (\partial \wedge B)) - j_e \cdot A - j_m \cdot B + \mathcal{L}_G. \quad (15)$$

The same result can also be obtained based on Schwinger's phenomenological source theory (PST) [47, 48]. PST introduces a source function to express the particles involved in a collision. The vacuum amplitude between two types of sources yields the  $S$  matrix element. For the theory of magnetic charge, based on PST, Ref. [49] showed the same photon action as Eq. (15) in the QEMD theory. Similarly, the Lagrangian of massive dark photons assumes the following form

$$\begin{aligned} \mathcal{L}_{DP} = & -\frac{1}{2n^2}[n \cdot (\partial \wedge A_D)] \cdot [n \cdot (\partial \wedge B_D)]^d \\ & + \frac{1}{2n^2}[n \cdot (\partial \wedge B_D)] \cdot [n \cdot (\partial \wedge A_D)]^d \\ & - \frac{1}{2n^2}[n \cdot (\partial \wedge A_D)]^2 - \frac{1}{2n^2}[n \cdot (\partial \wedge B_D)]^2 \\ & + \frac{1}{2}m_D^2 A_D^\mu A_{D\mu} + \frac{1}{2}m_D^2 B_D^\mu B_{D\mu} + \mathcal{L}_{GD} \\ = & \frac{1}{4}\text{tr}(F_D \cdot (\partial \wedge A_D)) + \frac{1}{4}\text{tr}(F_D^d \cdot (\partial \wedge B_D)) \\ & + \frac{1}{2}m_D^2 A_D^\mu A_{D\mu} + \frac{1}{2}m_D^2 B_D^\mu B_{D\mu} + \mathcal{L}_{GD}, \end{aligned} \quad (16)$$

where  $\mathcal{L}_{GD}$  denotes the gauge fixing term for DP.

Spatial vector  $n_\mu$  introduced in the QEMD theory seems to violate the Lorentz invariance. This originates from the non-locality of the QEMD theory. Brandt, Neri, and Zwanziger formally showed that the observables of the QEMD are the Lorentz invariant using the path-integral approach [30, 31] (see also a recent demonstration in Ref. [32]). They claimed that, after all the quantum corrections are properly accounted for, the dependence on spatial vector  $n_\mu$  in the action factorizes into an integer linking number multiplied by the combination of charges under the quantization condition,  $q_i g_j - q_j g_i$ . This  $n$ -dependent part is then given by  $2\pi$  multiplied by an integer. Since the action contributes to the generating functional in the exponential form, this Lorentz-violating part does not play any role in physical processes. According to Refs. [31, 49, 50], the kinetic and current terms can be rewritten as

$$\mathcal{L}_P \supset -\frac{1}{2}F \cdot (\partial \wedge A) + \frac{1}{4}F^2 - j_e \cdot A - j_m \cdot B_n, \quad (17)$$

where the redefined potential is  $B_n(x) = \int d\omega \cdot F^d(x - \omega) = (n \cdot \partial)^{-1} n \cdot F^d(x)$ . The action of the QEMD theory remains invariant under the combined gauge transformation and Lorentz transformation [30]

$$F \rightarrow F, A_\mu \rightarrow A_\mu + \partial_\mu \lambda, B_n \rightarrow B_{n'} = (n' \cdot \partial)^{-1} n' \cdot F^d, \quad (18)$$

where function  $\lambda(x)$  is determined by the following condition:

$$\partial \wedge \partial \lambda = \{[(n' \cdot \partial)^{-1} n' - (n \cdot \partial)^{-1} n] \wedge j_m\}^d. \quad (19)$$

The Lagrangian of massive DP gains two mass terms in addition to the conventional QEMD Lagrangian with the substitution of  $A \rightarrow A_D$  and  $B \rightarrow B_D$ . The DP Lagrangian can be obtained by combining two forms of Lagrangians

$$\begin{aligned} \mathcal{L}_{\text{DP1}} = & -\frac{1}{2} F_D \cdot (\partial \wedge A_D) + \frac{1}{4} F_D^2 \\ & - j_{eD} \cdot A_D - j_{mD} \cdot B_{Dn} + m_D^2 A_D^2, \end{aligned} \quad (20)$$

$$\begin{aligned} \mathcal{L}_{\text{DP2}} = & -\frac{1}{2} F_D^d \cdot (\partial \wedge B_D) + \frac{1}{4} F_D^{d2} \\ & - j_{eD} \cdot A_{Dn} - j_{mD} \cdot B_D + m_D^2 B_D^2, \end{aligned} \quad (21)$$

where  $\mathcal{L}_{\text{DP1}}$  ( $\mathcal{L}_{\text{DP2}}$ ) is composed of  $F_D$ ,  $A_D$ , and  $B_{Dn}$  ( $F_D^d$ ,  $B_D$  and  $A_{Dn}$ ). Analogous to  $\mathcal{L}_{\text{DP1}}$ ,  $\mathcal{L}_{\text{DP2}}$  can also be proved to be a Lorentz invariant [49]. Thus, the DP Lagrangian with mass terms satisfy Lorentz symmetry. We omit the dark currents in the following calculation.

### III. DARK PHOTON-PHOTON INTERACTIONS AND FIELD EQUATIONS

Inspired by the two potential terms in either  $\mathcal{L}_P$  or  $\mathcal{L}_{\text{DP}}$ , we can build the low-energy dark photon-photon kinetic mixing interactions as follows

$$\begin{aligned} \mathcal{L}_{\text{DP-P}} = & \frac{\epsilon_1}{2} \text{tr}(F \cdot (\partial \wedge A_D)) + \frac{\epsilon_1}{2} \text{tr}(F^d \cdot (\partial \wedge B_D)) \\ & + \frac{\epsilon_2}{2} \text{tr}(F^d \cdot (\partial \wedge A_D)) - \frac{\epsilon_2}{2} \text{tr}(F \cdot (\partial \wedge B_D)). \end{aligned} \quad (22)$$

This Lagrangian is equivalent to the one with the substitution of  $A \leftrightarrow A_D$  and  $B \leftrightarrow B_D$ . They contribute to the same equations of motion. The two mixing parameters,  $\epsilon_1$  and  $\epsilon_2$ , can be obtained by integrating out the new heavy fermion  $\psi$  in the vacuum polarization diagram of the potentials in the visible and dark sectors. Suppose fermion  $\psi$  is only charged in the  $U(1)_{A_D}$  group in the dark sector, the above Lagrangian can be simplified as

$$\mathcal{L}'_{\text{DP-P}} = \frac{\epsilon_1}{2} \text{tr}(F \cdot (\partial \wedge A_D)) + \frac{\epsilon_2}{2} \text{tr}(F^d \cdot (\partial \wedge A_D)), \quad (23)$$

where the terms with potential  $B_D$  in  $\mathcal{L}_{\text{DP-P}}$  vanish.

We next apply the Euler-Lagrange equation to the above DP-P Lagrangian  $\mathcal{L}_{\text{DP-P}}$  and then obtain the field equations of the photon as

$$\partial_\mu F^{\mu\nu} + \epsilon_1 \partial_\mu F_D^{\mu\nu} - \epsilon_2 \partial_\mu F_D^{d\mu\nu} = j_e^\nu, \quad (24)$$

$$\partial_\mu F^{d\mu\nu} + \epsilon_1 \partial_\mu F_D^{d\mu\nu} + \epsilon_2 \partial_\mu F_D^{\mu\nu} = j_m^\nu. \quad (25)$$

The equations of motion for the dark photon are

$$\partial_\mu F_D^{\mu\nu} + m_D^2 A_D^\nu + \epsilon_1 \partial_\mu F^{\mu\nu} + \epsilon_2 \partial_\mu F^{d\mu\nu} = 0, \quad (26)$$

$$\partial_\mu F_D^{d\mu\nu} + m_D^2 B_D^\nu + \epsilon_1 \partial_\mu F^{d\mu\nu} - \epsilon_2 \partial_\mu F^{\mu\nu} = 0. \quad (27)$$

After inserting the dark photon equations into Eqs. (24) and (25), we obtain the modified Maxwell's equations

$$\partial_\mu F^{\mu\nu} = \epsilon_1 m_D^2 A_D^\nu - \epsilon_2 m_D^2 B_D^\nu, \quad (28)$$

$$\partial_\mu F^{d\mu\nu} = \epsilon_1 m_D^2 B_D^\nu + \epsilon_2 m_D^2 A_D^\nu, \quad (29)$$

where the  $O(\epsilon_{1,2}^2)$  terms are neglected, and the primary electromagnetic fields driven by the static currents and charges have been subtracted. Note that the right-handed sides of Eqs. (28) and (29) are the linear combinations of  $A_D$  and  $B_D$ . We perform an  $O(2)$  transformation

$$\begin{pmatrix} \tilde{A}_D \\ \tilde{B}_D \end{pmatrix} = \begin{pmatrix} \cos \varphi & -\sin \varphi \\ \sin \varphi & \cos \varphi \end{pmatrix} \begin{pmatrix} A_D \\ B_D \end{pmatrix}, \quad (30)$$

where  $\cos \varphi = \epsilon_1 / \sqrt{\epsilon_1^2 + \epsilon_2^2}$  and  $\sin \varphi = \epsilon_2 / \sqrt{\epsilon_1^2 + \epsilon_2^2}$ . The equations then become

$$\partial_\mu F^{\mu\nu} = \epsilon m_D^2 \tilde{A}_D^\nu, \quad (31)$$

$$\partial_\mu F^{d\mu\nu} = \epsilon m_D^2 \tilde{B}_D^\nu, \quad (32)$$

where the only mixing parameter is  $\epsilon = \sqrt{\epsilon_1^2 + \epsilon_2^2}$ . The above Maxwell's equations can be simplified to correspond to Lagrangian  $\mathcal{L}'_{\text{DP-P}}$  as follows:

$$\partial_\mu F^{\mu\nu} = \epsilon_1 m_D^2 A_D^\nu, \quad (33)$$

$$\partial_\mu F^{d\mu\nu} = \epsilon_2 m_D^2 A_D^\nu, \quad (34)$$

where the dark sector has  $A_D$  only and the two equations

rely on  $\epsilon_1$  and  $\epsilon_2$ .

The modified Ampère's law and Faraday's law equations become

$$\vec{\nabla} \times \vec{\mathbb{B}} = \frac{\partial \vec{\mathbb{E}}}{\partial t} + \vec{j}_{eD}, \quad (35)$$

$$-\vec{\nabla} \times \vec{\mathbb{E}} = \frac{\partial \vec{\mathbb{B}}}{\partial t} + \vec{j}_{mD}, \quad (36)$$

where " $\mathbb{E}$ " and " $\mathbb{B}$ " denote the DP-induced electric and magnetic fields, respectively. After applying the curl differential operator to the above equations, one obtains two second-order differential equations

$$\vec{\nabla}^2 \vec{\mathbb{E}} - \frac{\partial^2 \vec{\mathbb{E}}}{\partial t^2} = \frac{\partial \vec{j}_{eD}}{\partial t} + \vec{\nabla} \times \vec{j}_{mD}, \quad (37)$$

$$\vec{\nabla}^2 \vec{\mathbb{B}} - \frac{\partial^2 \vec{\mathbb{B}}}{\partial t^2} = \frac{\partial \vec{j}_{mD}}{\partial t} - \vec{\nabla} \times \vec{j}_{eD}, \quad (38)$$

where we take  $A_D^0 = 0$  or  $\tilde{A}_D^0 = \tilde{B}_D^0 = 0$  and only keep their spatial components [4]. Next, we consider two cases for the dark currents corresponding to the above two types of Maxwell's equations

$$\text{case I: } \begin{cases} \vec{j}_{eD} = \epsilon_1 m_D^2 \vec{A}_D, \\ \vec{j}_{mD} = \epsilon_2 m_D^2 \vec{A}_D, \end{cases} \quad \text{case II: } \begin{cases} \vec{j}_{eD} = \epsilon m_D^2 \vec{A}_D, \\ \vec{j}_{mD} = \epsilon m_D^2 \vec{B}_D. \end{cases} \quad (39)$$

The two cases also correspond to a one-component ( $A_D$ ) DM scenario or two-component ( $\tilde{A}_D$  and  $\tilde{B}_D$ ) DM scenarios. In these two cases, the local DM density [51, 52] is given by

$$\rho_0 = 0.45 \text{ GeV cm}^{-3} = \begin{cases} \frac{1}{2} m_D^2 |\vec{A}_D|^2 & \text{case I,} \\ \frac{1}{2} m_D^2 (|\vec{A}_D|^2 + |\vec{B}_D|^2) & \text{case II.} \end{cases} \quad (40)$$

We adopt the scenario in Refs. [4, 7] to ensure that the dark photon field is along fixed direction  $\vec{k}$ . Consequently,  $\vec{\nabla} \times \vec{j}_{eD} = \vec{\nabla} \times \vec{j}_{mD} = 0$ . In case II, we define the ratio of two-component DM percentages as

$$\frac{|\vec{A}_D|^2}{|\vec{B}_D|^2} = \frac{x}{1-x}, \quad (41)$$

where  $0 < x < 1$ . Then, the DP DM fields can be expressed as follows

$$\text{case I: } \vec{A}_D = \frac{\sqrt{2\rho_0}}{m_D} e^{-im_D t} \hat{k},$$

$$\text{case II: } \begin{cases} \vec{A}_D = \frac{\sqrt{2\rho_0 x}}{m_D} e^{-im_D t} \hat{k}, \\ \vec{B}_D = \frac{\sqrt{2\rho_0(1-x)}}{m_D} e^{-im_D t} \hat{k}. \end{cases} \quad (42)$$

In case I, the DM density is composed of  $A_D$  only. The two second-order differential equations are governed by kinetic mixing parameters  $\epsilon_1$  and  $\epsilon_2$ , respectively. In case II, there is one free kinetic mixing parameter  $\epsilon$ . The two equations are induced by the two components of DM,  $\vec{A}_D$  and  $\vec{B}_D$ .

Note that the Lagrangian Eq. (22) satisfies  $SL(2, Z)$  symmetry, which ensures the theory's consistency under electromagnetic dual transformations. The symmetry implies that electric and magnetic charges can be interchanged under  $SL(2, Z)$  transformation, with the Lagrangian form remaining invariant. One can rewrite the general QEMD Lagrangian in differential notation [53]:

$$\begin{aligned} \mathcal{L}_P = & -\text{Im} \left\{ \frac{\tau}{8\pi n^2} [n \cdot \partial \wedge (\bar{A} + i\bar{B})] \cdot [n \cdot \partial \wedge (\bar{A} - i\bar{B})] \right\} \\ & -\text{Re} \left\{ \frac{\tau}{8\pi n^2} [n \cdot \partial \wedge (\bar{A} + i\bar{B})] \cdot [n \cdot (\partial \wedge (\bar{A} - i\bar{B}))^d] \right\} \\ & -\text{Re} \left\{ (\bar{A} - i\bar{B}) \cdot (J + \tau K) \right\}, \end{aligned} \quad (43)$$

where  $\tau$  is the modular group parameter of the  $SL(2, Z)$  symmetry,

$$\tau = \frac{\theta}{2\pi} + \frac{in_0}{e^2} \quad (44)$$

with  $n_0 = eg = 4\pi$ , and we neglect  $\theta$  below. We redefine  $\bar{A} \equiv eA$ ,  $\bar{B} \equiv eB$ ,  $J \equiv j_e/e$ , and  $K \equiv j_m e/4\pi$ . Under the  $SL(2, Z)$  duality transformation, parameter  $\tau$  and electromagnetic fields are transformed as [44]

$$\tau \rightarrow \tau' = \frac{a\tau + b}{c\tau + d}, \quad \text{Im}(\tau) \rightarrow \text{Im}(\tau') = \frac{\text{Im}(\tau)}{|c\tau + d|^2}, \quad (45)$$

$$\bar{A}_\mu + i\bar{B}_\mu \rightarrow \frac{1}{c\tau' + d} (\bar{A}'_\mu + i\bar{B}'_\mu), \quad (46)$$

$$\bar{A}_\mu - i\bar{B}_\mu \rightarrow \frac{1}{c\tau + d} (\bar{A}'_\mu - i\bar{B}'_\mu), \quad (47)$$

where integers  $a$ ,  $b$ ,  $c$ , and  $d$  are the matrix elements of  $SL(2, Z)$  transformation and satisfy  $ad - bc = 1$ . The electromagnetic tensors and currents follow the transformations [44]

$$\bar{F}_{\mu\nu} + i\bar{F}_{\mu\nu}^d \rightarrow \frac{1}{c\tau^* + d} (\bar{F}'_{\mu\nu} + i\bar{F}'_{\mu\nu}{}^d), \quad (48)$$

$$\bar{F}_{\mu\nu} - i\bar{F}_{\mu\nu}^d \rightarrow \frac{1}{c\tau + d} (\bar{F}'_{\mu\nu} - i\bar{F}'_{\mu\nu}{}^d), \quad (49)$$

$$J \rightarrow bK' + dJ', \quad K \rightarrow aK' + cJ'. \quad (50)$$

We can also rewrite our Lagrangian in Eq. (22) as

$$\begin{aligned} \mathcal{L}_{\text{DP-P}} = & -\frac{\text{Im}(\tau)}{4\pi} \left\{ \frac{\epsilon_1}{2} [\bar{F} \cdot (\partial \wedge \bar{A}_D) + \bar{F}^d \cdot (\partial \wedge \bar{B}_D)] \right. \\ & \left. + \frac{\epsilon_2}{2} [\bar{F}^d \cdot (\partial \wedge \bar{A}_D) + \bar{F} \cdot (\partial \wedge \bar{B}_D)] \right\}. \end{aligned} \quad (51)$$

The complete equation of motion is

$$\frac{\text{Im}(\tau)}{4\pi} \partial_\mu (\bar{F} + i\bar{F}^d) - \frac{\text{Im}(\tau)}{4\pi} m_D^2 (\epsilon_1 + i\epsilon_2) (\bar{A}_D + i\bar{B}_D) = J + \tau K. \quad (52)$$

Under  $SL(2, Z)$ , it then becomes

$$\frac{\text{Im}(\tau')}{4\pi} \partial_\mu (\bar{F}' + i\bar{F}'^d) - \frac{\text{Im}(\tau')}{4\pi} m_D^2 (\epsilon_1 + i\epsilon_2) (\bar{A}'_D + i\bar{B}'_D) = J' + \tau' K'. \quad (53)$$

#### IV. STRATEGY AND SENSITIVITY OF HALOSCOPE EXPERIMENTS

Next, we solve the above equations in terms of the DP DM fields and examine the detection strategies in a cavity haloscope experiment [4, 54] or an LC circuit experiment [7, 8]<sup>1)</sup>. Below, we take case II as an illustrative investigation and solve the two equations governed by  $\vec{A}_D$  and  $\vec{B}_D$ . The results of case I can be easily obtained by taking the substitution  $\epsilon \sqrt{x} \rightarrow \epsilon_1$  or  $\epsilon \sqrt{1-x} \rightarrow \epsilon_2$ .

For the direction of DP DM, we assume  $\theta$  as the angle between the direction  $\vec{k}$  of the DP field and the  $z$  direction in the laboratory coordinate system [4]. The direction  $\vec{k}$  of the DP field can be arbitrary. We must average the final result over all randomly pointing directions for  $\vec{k}$ .

##### A. Cavity haloscope

We first revisit the solution of Eq. (37) in case II for the cavity experiment. It has exactly the same Maxwell's equation as those induced by DP DM electrodynamics for the conventional cavity experiment.

Electric field  $\vec{\mathbb{E}}(t, \vec{x})$  in the microwave cavity can be

decomposed as the superposition of time-evolution functions  $e_n(t)$  and orthogonal modes  $\mathbb{E}_n(\vec{x})$

$$\vec{\mathbb{E}}(t, \vec{x}) = \sum_n e_n(t) \vec{\mathbb{E}}_n(\vec{x}), \quad (54)$$

where modes  $\vec{\mathbb{E}}_n(\vec{x})$  satisfy the Helmholtz equation  $\nabla^2 \vec{\mathbb{E}}_n + \omega_n^2 \vec{\mathbb{E}}_n = 0$  with resonant frequency  $\omega_n$  equal to the frequency of DP  $\omega_D \approx m_D$ . Plugging  $\vec{\mathbb{E}}(t, \vec{x})$  into Eq. (37) and considering the losses within the cavity, we obtain expansion coefficient  $e_n(t)$  as follows

$$\left( \frac{d^2}{dt^2} + \frac{\omega_D}{Q} \frac{d}{dt} + \omega_D^2 \right) e_n(t) = -\frac{\epsilon m_D^2}{C_n^{\mathbb{E}}} \int dV \vec{\mathbb{E}}_n^*(\vec{x}) \cdot \partial_t \vec{A}_D, \quad (55)$$

where the normalization coefficients are defined as  $C_n^{\mathbb{E}} = \int dV |\vec{\mathbb{E}}_n(\vec{x})|^2$  and  $Q$  denotes the quality factor. When assuming  $e_n(t) = e_{n,0} e^{-i\omega t}$ , coefficient  $e_{n,0}$  is given by

$$\begin{aligned} e_{n,0} = & \frac{\left( \omega_D^2 - \omega^2 + i \frac{\omega \omega_D}{Q} \right)}{\left( \omega_D^2 - \omega^2 \right)^2 + \frac{\omega^2 \omega_D^2}{Q^2}} \Big|_{\omega \approx \omega_D} \times \left( -\frac{\epsilon m_D^2}{C_n^{\mathbb{E}}} \right) \int dV \vec{\mathbb{E}}_n^* \cdot \partial_t \vec{A}_D \\ = & -i \frac{\epsilon Q}{C_n^{\mathbb{E}}} \times \int dV \vec{\mathbb{E}}_n^*(\vec{x}) \cdot \partial_t \vec{A}_D. \end{aligned} \quad (56)$$

The output power in the cavity can be obtained in terms of the energy stored in cavity  $U$  and the quality factor

$$\begin{aligned} P_{\text{DP}}^{\mathbb{E}} = & \kappa \frac{U}{Q} \omega_D = \kappa \frac{\omega_D}{Q} \frac{|e_{n,0}|^2}{2} \int dV |\vec{\mathbb{E}}_n(\vec{x})|^2 \\ = & \frac{\kappa}{2} \epsilon^2 m_D Q V |\partial_t \vec{A}_D|^2 G^{\mathbb{E}} \cos^2 \theta, \end{aligned} \quad (57)$$

where  $\kappa$  is the cavity coupling factor depending on the experimental setup,  $|\partial_t \vec{A}_D|^2 = 2\rho_0 x$ , and the form factor depending on the geometry of the cavity is

$$G^{\mathbb{E}} = \frac{\int dV \vec{\mathbb{E}}_n^*(\vec{x}) \cdot \vec{x}^2}{V \int dV |\vec{\mathbb{E}}_n(\vec{x})|^2}. \quad (58)$$

After averaging over all possible DP directions, compared to the axion cavity detection, the form factor here should be multiplied by  $\langle \cos^2 \theta \rangle = \int \cos^2 \theta d\Omega / \int d\Omega = 1/3$ .

For the detection of the DP field, similar to the axion search in cavity experiments, the  $\text{TM}_{010}$  mode has the largest coupling to DP with the electric field along the  $\vec{z}$ -

1) There is also detection strategy of vector DM using the Zeeman effect between atomic states [55].

axis. In this case, the theoretical value of the form factor for an ideal cylindrical cavity is  $G^{\mathbb{B}} \approx 0.69$  and the value for ADMX with tuning rods is  $G^{\mathbb{B}} \approx 0.455$  [52]. The signal power in axion cavity experiments can be derived as

$$P_{\text{axion}}^{\mathbb{B}} = \kappa \left[ g_{a\gamma\gamma}^2 \frac{|\mathbb{B}_0|^2}{m_a} \right] \rho_0 Q V G^{\mathbb{B}}, \quad (59)$$

where  $|\mathbb{B}_0|$  denotes the magnitude of the external static magnetic field. Taking  $P_{\text{DP}}^{\mathbb{B}} = P_{\text{axion}}^{\mathbb{B}}$  yields the following relation:

$$\epsilon^2 m_D x (\cos^2 \theta) = g_{a\gamma\gamma}^2 \frac{|\mathbb{B}_0|^2}{m_a}. \quad (60)$$

The constraints on the axion-photon coupling  $g_{a\gamma\gamma}$  from the existing axion cavity experiments can be converted to constrain parameter  $\epsilon\sqrt{x}$  for DP. Figure 1 shows the sensitivity of the cavity haloscope experiment to kinetic mixing  $\epsilon\sqrt{x}$  (or  $\epsilon_1$ ) as a function of  $m_D$ . For  $\epsilon\sqrt{x}$ , we show the converted limits (gray) from axion cavity experiments according to Eq. (60) as well as direct DP search limits (red) from WISPDMMX [9], SRF cavity [16], SQuAD [57], and APEX [17]. It is clear that the form of our Maxwell's equation Eq. (37) is exactly the same as the one for DP in QED. The induced power in the cavity in Eq. (57) is also similar to that in QED [4], except for the additional free DM fraction constant  $x$ . This is because we have two-component DP DM in the QEMD model ( $\tilde{A}_D$  and  $\tilde{B}_D$ ) unlike the QED case where one-component DP has 100% DM density. In other words, when  $x = 1$ , our analytical results for  $\tilde{A}_D$  restore the QED DP case. The spirit of the experimental setup for  $\tilde{A}_D$  should also be the same as that for QED DP. Thus,

the existing results of current DP cavity experiments can be directly applied to constrain our parameter combination  $\epsilon\sqrt{x}$  in case II (or  $\epsilon_1$  in our case I). The above WISPDMMX, SRF cavity, SQuAD, and APEX experiments searched for resonant DPs using a tunable radio frequency cavity or a superconducting radio frequency cavity with a high quality factor. They provide upper bounds on  $\epsilon\sqrt{x}$  for individual DP masses in the range of  $\sim 0.1 - 30 \mu\text{eV}$ . The SRF cavity with a remarkably high quality factor of about  $10^{10}$  yields the most stringent bound of  $\epsilon\sqrt{x} < 2 \times 10^{-16}$  at 1.3 GHz [16]. APEX uses high-performance amplifiers specifically designed for low-temperature environments, achieving an extremely low temperature compared to other experiments and effectively reducing background noise. It sets the parameter limit as  $\epsilon\sqrt{x} < 3.7 \times 10^{-13}$  around 7.139 GHz at 90% confidence level [17]. SQuAD employs superconducting qubit technology and sub-standard quantum limit (sub-SQL) detection techniques, further reducing noise and improving detection precision. Its background shot noise remains at 15.7 dB, providing a limit of  $\epsilon\sqrt{x} < 1.68 \times 10^{-15}$  at 6.011 GHz [57]. WISPDMMX employs four tuned resonant modes to scan for signals, enabling a probe over a broader mass range of  $0.22.07 \mu\text{eV}$  and achieving a sensitivity limit of  $\epsilon\sqrt{x} < 10^{-13} - 10^{-12}$  [9].

Similarly, we can follow the same procedure to obtain the solution of Eq. (38) for the emission power of magnetic field modes  $\vec{\mathbb{B}}_n(\vec{x})$  induced by  $\partial_t \vec{\mathbb{B}}_D$

$$P_{\text{DP}}^{\mathbb{B}} = \frac{\kappa}{2} \epsilon^2 m_D Q V |\partial_t \vec{\mathbb{B}}_D|^2 G^{\mathbb{B}} \cos^2 \theta = \kappa \epsilon^2 m_D (1-x) \rho_0 Q V G^{\mathbb{B}} \cos^2 \theta, \quad (61)$$

$$G^{\mathbb{B}} = \frac{|\int dV \vec{\mathbb{B}}_n^*(\vec{x}) \cdot \vec{x}|^2}{V \int dV |\vec{\mathbb{B}}_n(\vec{x})|^2}. \quad (62)$$

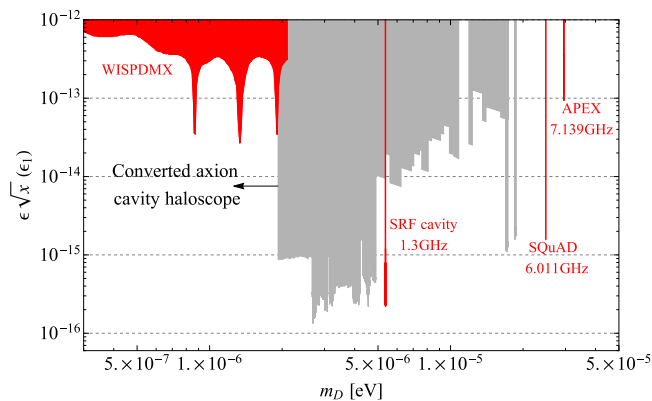


**Fig. 1.** (color online) Sensitivity of the cavity haloscope experiment to kinetic mixing  $\epsilon\sqrt{x}$  ( $\epsilon_1$ ). For the converted results in gray, we take the limits of axion coupling  $g_{a\gamma\gamma}$  from the AxionLimits repository [56]. The direct DP search limits from WISPDMMX [9], SRF cavity [16], SQuAD [57], and APEX [17] are also shown in red.

Next, we discuss the feasibility of DP field  $\vec{\mathbb{B}}_D$  detection. It turns out that one needs the magnetic field modes along the  $\vec{z}$ -axis, corresponding to the TE modes. In an ideal cylindrical cavity, the form factor of the TE<sub>011</sub> mode is canceled over the radial integral from 0 to the radius. The higher-order TE<sub>111</sub> mode exhibits periodic symmetry along the direction of azimuthal angle  $\phi$ . This causes the response to dark photon to be canceled over the integral from 0 to  $2\pi$ . To avoid the cancellation, taking the TE<sub>111</sub> mode for illustration, we require an imperfect symmetric field distribution over the azimuthal angle direction within the cavity. In the practical setup of yhr cavity experiment, tuning rods are placed within the cylindrical cavity in to tune the mode. For instance, in the ADMX experiment, two copper rods are put inside the cavity for frequency tuning. As indicated in Ref. [58], the tuning rods rotate around a fixed center and then the field distribution in the cavity transforms asymmetrically over a full

scan cycle. Here, a reasonable modification for the  $TE_{111}$  mode is to take only one half of the original cylindrical cavity. We then partially integrate the magnetic field and calculate the form factors. Specifically, after integrating the azimuthal angle from 0 to  $\pi$ , the analytical result of the form factor  $G^{\mathbb{B}}$  corresponding to the  $TE_{111}$  mode is  $(128/\pi^4 x'_{1,1}{}^2) \times (c_1^2/c_2) \approx 0.61$ , where  $c_1 = \int_0^{x'_{1,1}} dx x J_1(x)$  and  $c_2 = \int_0^{x'_{1,1}} dx x J_1^2(x)$  with  $x'_{m,n}$  being the  $n$ -th zero point of the first derivative of the Bessel function,  $J_m(x)$ . It is close to the form factor of the  $TM_{010}$  mode. We leave the detailed electromagnetic simulation for a future study.

### B. LC circuit

For the LC circuit experiment, the DP Maxwell's equations must be solved with electromagnetic shielding [8]. We take the shield as a conducting or superconducting hollow cylinder of radius  $R$  along the  $\hat{z}$  direction in cylindrical coordinates  $(\rho, \phi, z)$ . In our case, in the presence of  $\vec{j}_{eD}$  and  $\vec{j}_{mD}$ , both the induced electric field and magnetic field in the  $z$  direction would respectively be suppressed by the electromagnetic shielding. That is, the observed  $\vec{\mathbb{E}}$  and  $\vec{\mathbb{B}}$  fields should be solved under boundary conditions  $\hat{z} \cdot \vec{\mathbb{E}} = \hat{z} \cdot \vec{\mathbb{B}} = 0$  on the surface with  $\rho = R$  [8]. The  $\vec{\mathbb{B}}$  and  $\vec{\mathbb{E}}$  along the  $\phi$  direction generated by the currents then become the dominant observable fields inside the shield.

The DP field is projected to the  $z$  direction below; thus, we have  $\vec{j}_{eD} = \epsilon m_D \sqrt{2\rho_0 x} e^{-im_D t} \cos \theta \hat{z}$  and  $\vec{j}_{mD} = \epsilon m_D \sqrt{2\rho_0(1-x)} e^{-im_D t} \cos \theta \hat{z}$ . For current  $\vec{j}_{eD}$  induced by  $\vec{A}_D$ , we solve the following equations

$$\vec{\nabla}^2 \vec{\mathbb{E}} - \frac{\partial^2 \vec{\mathbb{E}}}{\partial t^2} = \frac{\partial \vec{j}_{eD}}{\partial t}, \quad (63)$$

$$\vec{\nabla} \times \vec{\mathbb{B}} = \frac{\partial \vec{\mathbb{E}}}{\partial t} + \vec{j}_{eD}. \quad (64)$$

The solutions of observables  $\vec{\mathbb{E}}$  and  $\vec{\mathbb{B}}$  become

$$\begin{aligned} \vec{\mathbb{E}}_{\text{obs}} &= -i\epsilon \sqrt{2\rho_0 x} \cos \theta e^{-im_D t} \left(1 - \frac{J_0(m_D \rho)}{J_0(m_D R)}\right) \hat{z} \\ &\approx i\epsilon \sqrt{2\rho_0 x} \cos \theta e^{-im_D t} m_D^2 (R^2 - \rho^2) \hat{z}, \end{aligned} \quad (65)$$

$$\begin{aligned} \vec{\mathbb{B}}_{\text{obs}} &= \epsilon \sqrt{2\rho_0 x} \cos \theta e^{-im_D t} \frac{J_1(m_D \rho)}{J_0(m_D R)} \hat{\phi} \\ &\approx \epsilon \sqrt{2\rho_0 x} \cos \theta e^{-im_D t} m_D \rho \hat{\phi}. \end{aligned} \quad (66)$$

For  $x \rightarrow 1$ , the solution in Ref. [8] is obtained. An adjustable LC circuit is put inside a hollow conducting shield, and the inducting coil is wrapped around the  $\phi$  direction of the conductor to receive the driving magnetic field. When the resonant frequency of the LC circuit is tuned to the DP oscillation frequency, the observable magnetic field produces a magnetic flux and consequent

current

$$\Phi_{\text{obs}} \approx Q\epsilon \sqrt{2\rho_0 x} \cos \theta m_D V, \quad I = \frac{\Phi_{\text{obs}}}{L}, \quad (67)$$

where  $Q \sim 10^6$  is the quality factor of the LC circuit,  $V$  is the volume of the inductor, and  $L$  is the inductance of the inducting coil. The signal power is then given by

$$\begin{aligned} P_{\text{signal}} &= \langle I^2 R_s \rangle \approx \frac{\rho_0 x Q \epsilon^2 \langle \cos^2 \theta \rangle m_D^3 V^2}{L} \\ &\approx \rho_0 x Q \epsilon^2 \langle \cos^2 \theta \rangle m_D^3 V^{5/3}, \end{aligned} \quad (68)$$

where  $R_s = L m_D / Q$  is the resistance. The solutions of electromagnetic fields in Eqs. (65) and (66) are analogous to those of DP in the QED case [8], except for the DM fraction constant,  $x$ . The signal power is also similar after it is multiplied by an additional  $x$  factor. One can thus arrange the same setup of LC circuit experiments here for  $\vec{A}_D$ . The existing limits of DP from QED experiments can be directly applied to constrain the parameter combination  $\epsilon \sqrt{x}$  in case II (or  $\epsilon_1$  in case I) of our QEMD model.

The equations for current  $\vec{j}_{mD}$  induced by  $\vec{B}_D$  are

$$\vec{\nabla}^2 \vec{\mathbb{B}} - \frac{\partial^2 \vec{\mathbb{B}}}{\partial t^2} = \frac{\partial \vec{j}_{mD}}{\partial t}, \quad (69)$$

$$-\vec{\nabla} \times \vec{\mathbb{E}} = \frac{\partial \vec{\mathbb{B}}}{\partial t} + \vec{j}_{mD}. \quad (70)$$

The solution is

$$\begin{aligned} \vec{\mathbb{B}}_{\text{obs}} &= -i\epsilon \sqrt{2\rho_0(1-x)} \cos \theta e^{-im_D t} \left(1 - \frac{J_0(m_D \rho)}{J_0(m_D R)}\right) \hat{z} \\ &\approx i\epsilon \sqrt{2\rho_0(1-x)} \cos \theta e^{-im_D t} m_D^2 (R^2 - \rho^2) \hat{z}, \end{aligned} \quad (71)$$

$$\begin{aligned} \vec{\mathbb{E}}_{\text{obs}} &= -\epsilon \sqrt{2\rho_0(1-x)} \cos \theta e^{-im_D t} \frac{J_1(m_D \rho)}{J_0(m_D R)} \hat{\phi} \\ &\approx -\epsilon \sqrt{2\rho_0(1-x)} \cos \theta e^{-im_D t} m_D \rho \hat{\phi}. \end{aligned} \quad (72)$$

In this case, a superconducting shield is placed outside the electromagnetic detector. The magnetic field in the  $z$  direction is suppressed owing to the superconducting Meissner effect. A wire loop is put inside the cylindrical hole of the superconducting shield to conduct the induction current [36]. The LC circuit is then connected to the wire loop to enhance the signal power. The induction current is

$$I = \frac{2\pi R \mathbb{E}_{\text{obs}}(R)}{R_s} = \frac{2\pi R^2 \epsilon \sqrt{2\rho_0(1-x)} \cos \theta m_D}{R_s}. \quad (73)$$

The signal power is then given by

$$P_{\text{signal}} = \langle I^2 R_s \rangle \approx \frac{\rho_0(1-x)Q\epsilon^2 \langle \cos^2 \theta \rangle m_D V^{4/3}}{L} \approx \rho_0(1-x)Q\epsilon^2 \langle \cos^2 \theta \rangle m_D V. \quad (74)$$

We adopt the cryogenic amplifier described in Ref. [59] to receive and amplify the signals. The thermal noise present in circuits can be estimated as

$$P_{\text{noise}} = \kappa_B T_N \sqrt{\frac{\Delta f}{\Delta t}}, \quad (75)$$

where  $\kappa_B$  is the Boltzmann constant,  $T_N$  is the noise temperature,  $\Delta f = f/Q$  is the detector bandwidth, and  $\Delta t$  is the observation time. Observation time was one week and two setup benchmarks of volume  $V$ , inductance  $L$ , and temperature  $T_N$  were taken for both cases. An adjustable capacitance with a minimal value of 50 pF was taken, which maximized frequency. To estimate the sensitivity of  $\epsilon \sqrt{x}$  or  $\epsilon \sqrt{1-x}$ , the signal-to-noise ratio (SNR) must satisfy

$$\text{SNR} = \frac{P_{\text{signal}}}{P_{\text{noise}}} > 3. \quad (76)$$

In Fig. 2, we show the sensitivity of the LC circuit to  $\epsilon \sqrt{x}$  ( $\epsilon_1$ ) (red) and  $\epsilon \sqrt{1-x}$  ( $\epsilon_2$ ) (blue). The search potential of  $\vec{B}_D$  is more promising than that of  $\vec{A}_D$  at low frequencies. Some exclusion limits for light DP DM are also shown, including DM Pathfinder (green) [60], ADMX SLIC (purple) [61], Dark E-Field Radio Experiment (orange) [62], and (gray) [63]. As previously stated, they can be applied to constrain our parameter combination  $\epsilon \sqrt{x}$  in case II (or  $\epsilon_1$  in case I). These experiments are sensitive to DP masses lower than approximately  $1 \mu\text{eV}$ . An early fixed-frequency superconducting resonator sets a simple exclusion limit on  $\epsilon \sqrt{x} > 1.5 \times 10^{-9}$  for  $\sim 2 \text{ neV}$  DPs [60]. The most recent Dark E-Field Radio experiment can place a 95% exclusion limit on  $\epsilon \sqrt{x}$  between  $6 \times 10^{-15}$  and  $6 \times 10^{-13}$  over the mass range of  $0.21 - 1.24 \mu\text{eV}$  [63]. The ADMX SLIC experiment uses a superconducting LC circuit to detect low-frequency light axions in strong magnetic fields (ranging from 4.5 T to 7.0 T). When rescaled for our DP-photon kinetic mixing parameter, its exclusion limit gives  $\epsilon \sqrt{x} < 10^{-10}$  in the sub  $0.2 \mu\text{eV}$  range [61].

### C. Connection to cosmology

Next, we briefly discuss the connection of DP DM to cosmology. There are a few plausible DP production mechanisms that may generate the correct abundance of DM in the early Universe. The most popular one is the

misalignment mechanism [64–66]. Ref. [3] verified that the misalignment mechanism for axions also applied to DP. Next, we will explore the evolution equation and energy density of QEMD DP in a cosmological context. For simplicity, we focus on the homogeneous solution of QEMD DP fields with  $\partial_i A_{D\mu} = \partial_i B_{D\mu} = 0$ . In an expanding universe, we adopt the metric as  $\text{diag}(1, -a^2, -a^2, -a^2)$ , with  $a(t)$  being the scale factor. We define the following anti-symmetric tensors

$$G_{\alpha\beta} = F_{D\alpha\beta} + \epsilon_1 F_{\alpha\beta} + \epsilon_2 F_{\alpha\beta}^d, \quad K_{\alpha\beta} = \epsilon_1 F_{D\alpha\beta} - \epsilon_2 F_{D\alpha\beta}^d, \quad (77)$$

$$\bar{G}_{\alpha\beta} = G_{\alpha\beta}/a^2(t), \quad \bar{K}_{\alpha\beta} = K_{\alpha\beta}/a^2(t), \quad (78)$$

where  $\epsilon_1$  and  $\epsilon_2$  are the two DP-photon mixing couplings. Under these conventions, we can write down the evolution equations for the QEMD DP fields in the Universe as

$$\partial_0 G_{0\beta} + 3HG_{0\beta} - \partial_i \bar{G}_{i\beta} + m_D^2 A_{D\beta} = 0, \quad (79)$$

$$\partial_0 G_{0\beta}^d + 3HG_{0\beta}^d - \partial_i \bar{G}_{i\beta}^d + m_D^2 B_{D\beta} = 0, \quad (80)$$

where  $H$  denotes the Hubble parameter and we neglect the effect of non-minimal coupling(s) to gravity without changing the conclusion [4]. The corresponding energy density is given by

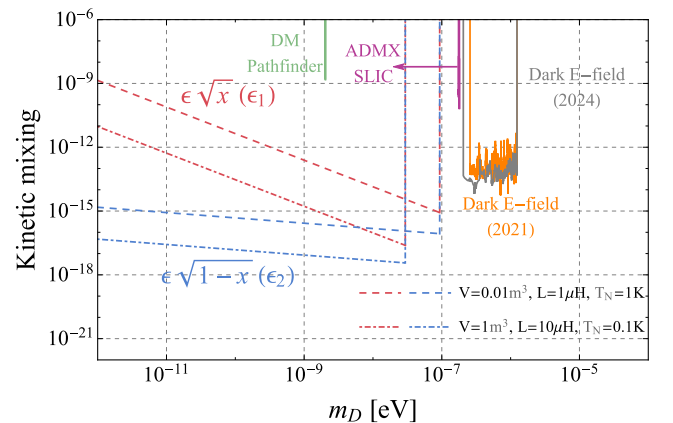


**Fig. 2.** (color online) Sensitivity of the LC circuit to kinetic mixings  $\epsilon \sqrt{x}$  ( $\epsilon_1$ ) (red) and  $\epsilon \sqrt{1-x}$  ( $\epsilon_2$ ) (blue). We assume two setup benchmarks for both cases. Some existing limits for light DP DM are also shown, including DM Pathfinder (green) [60], ADMX SLIC (purple) [61], Dark E-Field Radio Experiment (orange) [62], and (gray) [63].

$$\begin{aligned}
\rho(t) = T_0^0 = & -(\epsilon_1 F_D^{0i} - \epsilon_2 F_D^{d0i})(\partial_0 A_i) - (F_D^{0i} + \epsilon_1 F^{0i} + \epsilon_2 F^{d0i}) \\
& \times (\partial_0 A_{Di}) - (\epsilon_1 F_D^{d0i} + \epsilon_2 F_D^{0i})(\partial_0 B_i) - (F_D^{d0i} + \epsilon_1 F^{d0i} \\
& - \epsilon_2 F^{0i})(\partial_0 B_{Di}) - \mathcal{L}_{\text{DP}} - \mathcal{L}_{\text{DP-P}} = -K^{0i}(\partial_0 A_i) \\
& - G^{0i}(\partial_0 A_{Di}) - K^{d0i}(\partial_0 B_i) - G^{d0i}(\partial_0 B_{Di}) - \mathcal{L}_{\text{DP}} - \mathcal{L}_{\text{DP-P}} \\
= & \bar{K}_{0i} \dot{A}_i + \bar{G}_{0i} \dot{A}_{Di} + \bar{K}_{0i}^d \dot{B}_i + \bar{G}_{0i}^d \dot{B}_{Di} - \mathcal{L}_{\text{DP}} - \mathcal{L}_{\text{DP-P}}.
\end{aligned} \tag{81}$$

It is easy to prove that the above results can reduce to that of QED DP when the  $B$  and  $B_D$  fields vanish. This consistency indicates that the QEMD DP model is a reasonable extension of QED DP in cosmology. As a result, the energy density of DP behaves as non-relativistic matter with  $\rho(t) \propto 1/a^3(t)$  [4].

Another scenario of DP DM production is through quantum fluctuations during inflation [5]. Additionally, DP DM can be produced from the decay of topological defects such as cosmic strings [67]. This work focuses on the low-energy dynamics of DP and laboratory detection. One assumes that the DM distribution around the Earth is comprised of a cold population of DPs. A very detailed cosmological study of the QEMD DP is beyond the scope of this work, and we leave a dedicated study for the future.

## V. CONCLUSIONS

Dark matter and magnetic monopoles are two long-standing candidates of new physics beyond the SM. The ultralight dark photon is an intriguing bosonic dark matter. The interaction between the visible photon and dark photon is introduced by the gauge kinetic mixing between the field strength tensors of the SM electromagnetic gauge group and dark Abelian gauge group. Further, the relativistic electrodynamics was generalized to quantum electromagnetodynamics in the presence of both electric

and magnetic charges. In the QEMD theory, the physical photon is described by two four-potentials  $A_\mu$  and  $B_\mu$  corresponding to two  $U(1)$  gauge groups  $U(1)_A \times U(1)_B$ .

In this work, we construct the low-energy dark photon-photon interactions in the framework of QEMD. We introduce new heavy fermions charged under  $U(1)_A \times U(1)_B$  in the visible sector and  $U(1)_{A_D} \times U(1)_{B_D}$  in the dark sector. After integrating out the new fermions in vacuum polarization diagrams, the new dark photon-photon kinetic mixing interactions can be obtained. We derive the consequent field equations and the new Maxwell's equations in this framework. We also investigate the detection strategies of light dark photon DM as well as the generic kinetic mixings in cavity haloscope experiments and LC circuit experiments.

Finally, we give a detailed comparison between the DPs in QEMD and those in QED. Unlike QED, where each gauge field corresponds to either a visible photon or a DP, the QEMD framework introduces two Abelian gauge fields in both the visible and dark sectors. Consequently, the low-energy DP-photon Lagrangian in QEMD includes two kinetic mixing interactions, as opposed to the single interaction in the conventional DP theory. The presence of two gauge fields for DPs also enables a two-component dark matter scenario, characterized by  $\tilde{A}_D$  and  $\tilde{B}_D$ , with a single kinetic mixing parameter but different DM fraction constants. From the solutions of the new DP Maxwell's equations, one of the two DM components ( $\tilde{A}_D$ ) resembles the QED DP but includes an additional free DM fraction constant,  $x$ . The other DP component ( $\tilde{B}_D$ ) is essentially new, and its detection requires entirely new strategies in cavity and LC circuit experiments as we proposed in this article.

## ACKNOWLEDGMENTS

*We would like to thank Yu Gao for useful discussions.*

## References

- [1] B. Holdom, *Phys. Lett. B* **166**, 196 (1986)
- [2] B. Holdom, *Phys. Lett. B* **178**, 65 (1986)
- [3] A. E. Nelson and J. Scholtz, *Phys. Rev. D* **84**, 103501 (2011), arXiv: 1105.2812[hep-ph]
- [4] P. Arias, D. Cadamuro, M. Goodsell *et al.*, *JCAP* **06**, 013 (2012), arXiv: 1201.5902[hep-ph]
- [5] P. W. Graham, J. Mardon, and S. Rajendran, *Phys. Rev. D* **93**, 103520 (2016), arXiv: 1504.02102[hep-ph]
- [6] M. Fabbrichesi, E. Gabrielli, and G. Lanfranchi, *The Physics of the Dark Photon*, (2020), arXiv: 2005.01515 [hep-ph]
- [7] P. Arias, A. Arza, B. Döbrich *et al.*, *Eur. Phys. J. C* **75**, 310 (2015), arXiv: 1411.4986[hep-ph]
- [8] S. Chaudhuri, P. W. Graham, K. Irwin *et al.*, *Phys. Rev. D* **92**, 075012 (2015), arXiv: 1411.7382[hep-ph]
- [9] L. H. Nguyen, A. Lobanov, and D. Horns, *JCAP* **10**, 014 (2019), arXiv: 1907.12449[hep-ex]
- [10] R. Cervantes *et al.*, *Phys. Rev. D* **106**, 102002 (2022), arXiv: 2204.09475[hep-ex]
- [11] R. Cervantes, C. Braggio, B. Giaccone *et al.*, (2022), arXiv: 2208.03183 [hep-ex]
- [12] B. T. McAllister, A. Quiskamp, C. A. J. O'Hare *et al.*, *Annalen Phys.* **536**, 2200622 (2024), arXiv: 2212.01971 [hep-ph]
- [13] R. Cervantes *et al.*, *Phys. Rev. Lett.* **129**, 201301 (2022), arXiv: 2204.03818[hep-ex]
- [14] K. Ramanathan, N. Klimovich, R. Basu Thakur *et al.*, *Phys. Rev. Lett.* **130**, 231001 (2023), arXiv: 2209.03419[astro-ph.CO]
- [15] T. Schneemann, K. Schmieden, and M. Schott, (2023), arXiv: 2308.08337 [hep-ex]
- [16] Z. Tang *et al.* (SHANHE), *Phys. Rev. Lett.* **133**, 021005

- (2024), arXiv: 2305.09711[hep-ex]
- [17] D. He *et al.* (APEX), *Phys. Rev. D* **110**, L021101 (2024), arXiv: 2404.00908[hep-ex]
- [18] P. A. M. Dirac, *Proc. Roy. Soc. Lond. A* **133**, 60 (1931)
- [19] T. T. Wu and C. N. Yang, *Phys. Rev. D* **12**, 3845 (1975)
- [20] G. 't Hooft, *Nucl. Phys. B* **79**, 276 (1974)
- [21] A. M. Polyakov, *JETP Lett.* **20**, 194 (1974)
- [22] Y. M. Cho and D. Maison, *Phys. Lett. B* **391**, 360 (1997), arXiv: hep-th/9601028
- [23] P. Q. Hung, *Nucl. Phys. B* **962**, 115278 (2021), arXiv: 2003.02794[hep-ph]
- [24] J. Alexandre and N. E. Mavromatos, *Phys. Rev. D* **100**, 096005 (2019), arXiv: 1906.08738[hep-ph]
- [25] J. Ellis, N. E. Mavromatos, and T. You, *Phys. Lett. B* **756**, 29 (2016), arXiv: 1602.01745[hep-ph]
- [26] G. Lazarides and Q. Shafi, *Phys. Rev. D* **103**, 095021 (2021), arXiv: 2102.07124[hep-ph]
- [27] J. S. Schwinger, *Phys. Rev.* **144**, 1087 (1966)
- [28] D. Zwanziger, *Phys. Rev.* **176**, 1489 (1968)
- [29] D. Zwanziger, *Phys. Rev. D* **3**, 880 (1971)
- [30] R. A. Brandt, F. Neri, and D. Zwanziger, *Phys. Rev. Lett.* **40**, 147 (1978)
- [31] R. A. Brandt, F. Neri, and D. Zwanziger, *Phys. Rev. D* **19**, 1153 (1979)
- [32] A. V. Sokolov and A. Ringwald, *Annalen Phys.* **2023**, (2023), arXiv: 2303.10170 [hep-ph]
- [33] A. V. Sokolov and A. Ringwald, (2022), arXiv: 2205.02605 [hep-ph]
- [34] B. Heidenreich, J. McNamara, and M. Reece, *JHEP* **01**, 120 (2024), arXiv: 2309.07951[hep-ph]
- [35] T. Li and R. J. Zhang, (2023), arXiv: 2312.01355 [hep-ph]
- [36] T. Li, R. J. Zhang, and C. J. Dai, *JHEP* **03**, 088 (2023), arXiv: 2211.06847 [hep-ph]
- [37] M. E. Tobar, C. A. Thomson, B. T. McAllister *et al.*, *Annalen Phys.* **536**, 2200594 (2024), arXiv: 2211.09637 [hep-ph]
- [38] T. Li, C. J. Dai, and R. J. Zhang, *Phys. Rev. D* **109**, 015026 (2024), arXiv: 2304.12525 [hep-ph]
- [39] T. Li and R. J. Zhang, *Chin. Phys. C* **47**, 123104 (2023), arXiv: 2305.01344[hep-ph]
- [40] M. E. Tobar, A. V. Sokolov, A. Ringwald *et al.*, *Phys. Rev. D* **108**, 035024 (2023), arXiv: 2306.13320[hep-ph]
- [41] A. Patkos, *Mod. Phys. Lett. A* **38**, 2350137 (2023), arXiv: 2309.05523[hep-ph]
- [42] C. J. Dai, T. Li, and R. J. Zhang, (2024), arXiv: 2401.14195 [hep-ph]
- [43] A. Hook and J. Huang, *Phys. Rev. D* **96**, 055010 (2017), arXiv: 1705.01107[hep-ph]
- [44] J. Terning and C. B. Verhaaren, *JHEP* **12**, 123 (2018), arXiv: 1808.09459[hep-th]
- [45] J. Terning and C. B. Verhaaren, *JHEP* **12**, 152 (2019), arXiv: 1906.00014[hep-ph]
- [46] J. Terning and C. B. Verhaaren, *JHEP* **12**, 153 (2020), arXiv: 2010.02232[hep-th]
- [47] J. Schwinger, *Phys. Rev.* **152**, 1219 (1966)
- [48] J. S. Schwinger, *Phys. Rev.* **158**, 1391 (1967)
- [49] J. S. Schwinger, *Phys. Rev.* **173**, 1536 (1968)
- [50] T. m. Yan, *Phys. Rev.* **150**, 1349 (1966)
- [51] M. S. Turner, *Phys. Rev. D* **42**, 3572 (1990)
- [52] C. Bartram *et al.* (ADMX), *Phys. Rev. Lett.* **127**, 261803 (2021), arXiv: 2110.06096[hep-ex]
- [53] C. Csaki, Y. Shirman, and J. Terning, *Phys. Rev. D* **81**, 125028 (2010), arXiv: 1003.0448[hep-th]
- [54] Q. Yang, Y. Gao, and Z. Peng, *Commun. Phys.* **7**, 277 (2024), arXiv: 2201.08291[hep-ph]
- [55] Q. Yang and H. Di, *Phys. Lett. B* **780**, 622 (2018), arXiv: 1606.01492[hep-ph]
- [56] C. O'Hare, Cajohare/Axionlimits: Axionlimits, <https://cajohare.github.io/AxionLimits/> (2020)
- [57] A. V. Dixit, S. Chakram, K. He *et al.*, *Phys. Rev. Lett.* **126**, 141302 (2021), arXiv: 2008.12231[hep-ex]
- [58] T. Braine *et al.* (ADMX), *Phys. Rev. Lett.* **124**, 101303 (2020), arXiv: 1910.08638[hep-ex]
- [59] J. Duan, Y. Gao, C. Y. Ji *et al.*, *Phys. Rev. D* **107**, 015019 (2023), arXiv: 2206.13543[hep-ph]
- [60] A. Phipps *et al.*, *Springer Proc. Phys.* **245**, 139 (2020), arXiv: 1906.08814 [astro-ph.CO]
- [61] N. Crisosto, P. Sikivie, N. S. Sullivan *et al.*, *Phys. Rev. Lett.* **124**, 241101 (2020), arXiv: 1911.05772[astro-ph.CO]
- [62] B. Godfrey *et al.*, *Phys. Rev. D* **104**, 012013 (2021), arXiv: 2101.02805[physics.ins-det]
- [63] J. Levine, B. Godfrey, J. A. Tyson *et al.*, (2024), arXiv: 2405.20444 [hep-ex]
- [64] J. Preskill, M. B. Wise, and F. Wilczek, *Phys. Lett. B* **120**, 127 (1983)
- [65] L. F. Abbott and P. Sikivie, *Phys. Lett. B* **120**, 133 (1983)
- [66] M. Dine and W. Fischler, *Phys. Lett. B* **120**, 137 (1983)
- [67] A. J. Long and L. T. Wang, *Phys. Rev. D* **99**, 063529 (2019), arXiv: 1901.03312[hep-ph]